TRPC7 facilitates cell growth and migration by regulating intracellular Ca^{2+} mobilization in lung adenocarcinoma cells

JUI-LIN LIANG[1,2], MING-HSIEN TSAI[3], YI-CHUN HSIEH[4], HUEI-SYUAN LIU[4], SHAO-WEI CHEN[5], YUNG-YUN HUANG[6], LI-CHING LIN[7], TSUNG-FU TSAI[8], YUN-FANG LIANG[9] and WEN-LI HSU[4,10]

[1]Institute of Clinical Medicine, National Cheng Kung University College of Medicine, Tainan 701401; [2]Department of Surgery, Chi-Mei Medical Center, Liouying, Tainan 73657; [3]Department of Child Care, National Pingtung University of Science and Technology, Pingtung 91201; [4]Regenerative Medicine and Cell Therapy Research Center; [5]Department of Clinical Education and Training, Chung-Ho Memorial Hospital, Kaohsiung Medical University, Kaohsiung 80708; [6]Department of Anesthesiology, Kaohsiung Veterans General Hospital, Kaohsiung 813414; [7]Division of General Surgery; [8]Department of Dermatology, Chang Gung Memorial Hospital, New Taipei 33303; [9]School of Medicine, College of Medicine, Kaohsiung Medical University, Kaohsiung 80708; [10]Department of Dermatology, Kaohsiung Municipal Ta-Tung Hospital, Kaohsiung Medical University Hospital, Kaohsiung Medical University, Kaohsiung 80145, Taiwan, R.O.C.

Received August 2, 2022; Accepted December 15, 2022

DOI: 10.3892/ol.2023.13678

Abstract. Transient receptor potential canonical 7 (TRPC7) has been reported to mediate aging-associated tumorigenesis, but the role of TRPC7 in cancer malignancy is still unclear. TRPC7 is associated with tumor size in patients with lung adenocarcinoma and the present study further evaluated the underlying mechanism of TRPC7 in the regulation of cancer progression. The clinicopathological role of TRPC7 was assessed using immunohistochemistry staining and the pathological mechanism of TRPC7 in lung adenocarcinoma cells was determined using cell cycle examination, invasion and calcium response assays, and immunoblot analysis. The results indicated that high TRPC7 expression was associated with a lower 5-year survival rate compared with low TRPC7 expression, which suggested that TRPC7 expression was inversely associated with overall survival in patients with lung adenocarcinoma. TRPC7 serves a pathological role by facilitating the enhancement of cell growth and migration with increased phosphorylation of Ca^{2+}/calmodulin-dependent protein kinase II, AKT and ERK. TRPC7 knockdown in lung adenocarcinoma cells restrained cell cycle progression and cell migration by interrupting the TRPC7-mediated Ca^{2+} signaling-dependent AKT and MAPK signaling pathways. These findings demonstrated for the first time a role of oncogenic TRPC7 in the regulation of cancer malignancy and could provide a novel therapeutic molecular target for patients with lung adenocarcinoma.

Correspondence to: Dr Wen-Li Hsu, Department of Dermatology, Kaohsiung Municipal Ta-Tung Hospital, Kaohsiung Medical University Hospital, Kaohsiung Medical University, 68 Jhong Hua 3rd Road, Cianjin, Kaohsiung 80145, Taiwan, R.O.C.
E-mail: 1098129@kmuh.org.tw

Key words: transient receptor potential canonical 7, cancer cell growth, cancer cell migration, Ca^{2+} signaling, lung adenocarcinoma

Introduction

Ca^{2+} signaling is an important regulator of pathways involved in the regulation of cancer progression through oncogenic activation, including cell growth, metastasis and chemotherapy resistance (1). The involvement of cell signaling pathways, such as MAPK and PI3K/AKT, in the promotion of malignancy in cancer cells is Ca^{2+} dependent (2,3). Ca^{2+}-dependent activation of Ca^{2+}/calmodulin-dependent protein kinase II (CaMKII) contributes to the phosphorylation of AKT and ERK, and the Ca^{2+}/CaMKII/AKT and Ca^{2+}/CaMKII/ERK axes may be involved in governing cancer progression (4).

Recently, transient receptor potential (TRP) channels were reported to be associated with the development and progression of cancer (5). Ca^{2+} signaling from nociceptive TRP channels controls cancer pathophysiology (6) and the therapeutic targeting of TRP channels provides a novel approach for the treatment of cancer. A previous study also reported that TRP canonical 7 (TRPC7) mediates aging-associated tumorigenesis (7). Activation of the TRPC7-induced DNA damage response (DDR) triggers the senescence inflammation response and senescence-associated secretory phenotype activation, and genomic instability results in the activation of oncogenes and the dysfunction of tumor suppressor genes (7). Ca^{2+} signaling from TRPC7 is therefore involved in the initiation of tumorigenesis, but the role of TRPC7 in the regulation of cancer progression and malignancy is still unclear.

According to the results of our previous study, the pathologic features of TRPC7 were associated with tumor size in patients with lung adenocarcinoma (7). Lung adenocarcinoma falls under the umbrella of non-small cell lung cancer (NSCLC), which is the most common type of lung cancer

(accounting for ~85% of lung cancer cases) and the majority of patients with lung adenocarcinoma exhibit metastatic disease or local recurrence after surgery (8). The expression of TRPCs, especially TRPC1, 3, 4 and 6, have been reported to be associated with lung cancer differentiation (9) and TRPC7 may be involved in the regulation of lung cancer growth. Therefore, it could be hypothesized that TRPC7 promotes cancer progression via Ca^{2+}-mediated CaMKII, MAPK and AKT signaling pathways. The present study evaluated the role of TRPC7 in lung cancer progression. The association of TRPC7 with the overall survival rate of patients with lung adenocarcinoma was evaluated and the functional role of TRPC7 in regulating cancer malignancy was assessed.

Materials and methods

Patients and tumor specimens. Between January 2013-December 2016 there were 521 newly diagnosed lung adenocarcinoma in Chi-Mei Medical Center, Liouying. A total of 93 patients received curative thoracic surgery for tumor eradication. A total of 43 patients were excluded from the present study due to coexisting malignancy, previous neoadjuvant therapy, death within one month after operation and those who did not want to participate in this study. Finally, the remaining 50 patients were enrolled into the present study. Because seven patients were lost to follow up after surgery, only 43 patients had complete information for calculation of their 5-year survival rate. A total of 12 patients were randomly selected for examination of the protein expression levels of TRPC7 in their paired lung adenocarcinoma tissues and non-tumor tissues. Written informed consent was obtained from each patient and tissue specimens were processed according to protocols approved by the Institutional Review Board/Ethics Committee of Chi-Mei Medical Center (approval no. 10405-L01) for the study 'A potential oncogene gene, TRPC7 in NSCLS study'. The mean age of patients was 68 years (range, 38-88 years). The overall survival time after tumor removal was 55 months (range, 2-177 months). Specimens from these patients were received from the Department of Surgery at Chi-Mei Medical Center, and paired lung tumor and adjacent normal tissue were used in the present study were collected from these patient specimens. The clinicopathological characteristics of the patients were assessed according to the American Joint Committee on Cancer 7th edition lung cancer staging system (10).

Immunohistochemistry staining. Paraffin sections (3 μm) from the samples were incubated in a Thermotank set at 60˚C, for 20 min. Tissue sections were then immersed in 100% xylene for 10 min, and then in a graded (100, 90 and 75%) alcohol solution, each for 1-3 min. The sections were finally immersed in distilled water for 3 min. The high-pressure antigen retrieval was in sodium citrate buffer (pH 6) for 2 min at 100˚C. Bovine serum albumin (BSA; 5%; Sigma-Aldrich; Merck KGaA) in phosphate buffered saline (PBS; Sigma-Aldrich; Merck KGaA) was added to block the activity of the endogenous peroxidase. The samples were then incubated at room temperature for 1 h. An antibody against TRPC7 (antibody information and dilution ratio are presented in Table S1) was used to assess the expression of target molecule and the samples were incubated overnight at 4˚C. Immunoreactivity was visualized after incubation using the 3,3'-diaminobenzidine substrate-chromogen system (Dako Omnis; Agilent Technologies, Inc.) according to the manufacturer's protocol. The samples were imaged using an Axi-oPlan 2 bright field microscope (Zeiss AG). The staining intensity of TRPC7 was assessed using the ImageJ IHC Profiler plugin (11) for ImageJ (National Institutes of Health). After analysis of each image using the software, the image was automatically assigned a score as positive (++), low positive (+) or negative (-), which was dependent on its color deconvolution and computerized pixel profiling (11). Depending on the score, TRPC7 expression was classified as high expression (++) or low expression (+ and -).

Cell culture and plasmid transfection. The IMR-90, BEAS-2B, BES-1A1.6, H1299, A549 and H520 cell lines were purchased from the American Type Culture Collection. H125 and the primary normal human epidermal keratinocytes (cat. no. C-12005) were purchased from Creative Biolabs, Inc. and PromoCell GmbH., respectively. The IMR-90 human lung fibroblast, BEAS-2B human bronchial epithelium, BES-1A1.6 human bronchial epithelium and H125 human lung squamous cell carcinoma cell lines were cultured in DMEM (Gibco; Thermo Fisher Scientific, Inc.), and the H1299 human lung adenocarcinoma, A549 human lung adenocarcinoma and H520 human lung squamous cell carcinoma cells were cultured in RPMI 1640 (Gibco; Thermo Fisher Scientific, Inc.). All cell lines were maintained in RPMI 1640 or DMEM supplemented with 1% penicillin/streptomycin and 10% fetal bovine serum (FBS; Gibco; Thermo Fisher Scientific, Inc.). The primary normal human epidermal keratinocytes were cultured in serum-free keratinocyte growth medium (Gibco; Thermo Fisher Scientific, Inc.) supplemented with 0.005 μg/ml recombinant human epidermal growth factor, 0.05 mg/ml bovine pituitary extract and 5 μg/ml recombinant human insulin (all Gibco; Thermo Fisher Scientific, Inc.). All cells were incubated at 37˚C in a humidified incubator with 5% CO_2.

The pCMV3-TRPC7-GFPSpark plasmid encoding N-GFPSpark-tagged human TRPC7 (cat. no. HG15975-ACG) was purchased from Sino Biological, Inc. The TRPC7 sequence was cloned into the pCMV3-N-GFPSpark vector to generate the expression vector pCMV3-TRPC7-GFPSpark, which expressed a GFP-tagged TRPC7 fusion protein. The BEAS-2B cells were seeded into six-well plates at $4.5x10^5$ cells/well. The cells were then transfected with 1 μg pCMV3-TRPC7-GFPSpark using TransIT-X2® Dynamic Delivery System (Mirus Bio, Inc.). After 48 h incubation at 37˚C in a humidified incubator with 5% CO_2, cells were collected for use in cell cycle analysis, invasion assay and calcium response assay. For immunoblot analysis, TRPC7-overexpressing BEAS-2B (or H1299) cells were further treated with TRPC7 inhibitors, 5 μM SKF96365 (Sigma-Aldrich; Merck KGaA), 20 μM 2-aminoethyl diphenylborinate (2-APB, Sigma-Aldrich; Merck KGaA) or DMSO control for 24 h. The empty pCMV3-GFPSpark vector was used as a transfection control.

TRPC7 knockdown in lung cancer cells. For TRPC7 knockdown experiments using small interfering RNAs (siRNAs), H1299 cells were transfected with si TRPC7 (sc-106641; Santa Cruz Biotechnology, Inc.) or si control

(sc-37007; Santa Cruz Biotechnology, Inc) constructs using GenMute™ siRNA Transfection Reagent (SignaGen Laboratories), as previously described (7). After transfection, cells were cultured for 48 h at 37˚C in a humidified incubator with 5% CO_2 before undergoing further analyses. The expression of target genes was validated using immunoblot analysis.

Reverse transcription-quantitative PCR (RT-qPCR). After transfection with the siRNAs (si control and si TRPC7) or the plasmids (pCMV3-GFPSpark and pCMV3-TRPC7-GFPSpark) for 24 h, total RNA was extracted from cells utilizing TRIzol™ reagent (Thermo Fisher Scientific, Inc.). Complementary DNA was synthesized from RNA (1 μg) utilizing a RevertAid RT Reverse Transcription Kit (Thermo Fisher Scientific, Inc.). Incubation conditions were 10 min at 25˚C, 120 min at 37˚C, and 5 min at 85˚C. The resulting complementary DNAs were used to identify the expression of *TRPC7* and *GAPDH* by performing qPCR with a TaqMan™ Gene Expression Assay kit (Thermo Fisher Scientific, Inc.) and the following assay IDs, Hs00220638_m1 (*TRPC7*) and Hs02758991_g1 (*GAPDH*). According to the manufacturer's protocol, incubation conditions were 2 min at 50˚C, 10 min at 95˚C, and or 40 cycles for 15 sec at 95˚C and 1 min at 60˚C using a 7500 Fast Real-Time PCR System (Thermo Fisher Scientific; Inc.). The mRNA expression level of *TRPC7* was measured by the cycle threshold value quantification and normalization, using the $2^{-\Delta\Delta Cq}$ method and compared with the GAPDH (12).

Immunoblot analysis. Ground tissues or cells were lysed by incubation on ice for 30 min in M-PER® Mammalian Protein Extraction Reagent (Thermo Fisher Scientific, Inc.) containing proteinase (cat. no. S8830-20TAB; Sigma-Aldrich; Merck KGaA) and phosphatase inhibitors (cat. no. 5870S; Cell Signaling Technology, Inc.). Cell debris were removed by centrifugation at 14,000 x g for 30 min at 4˚C. The protein concentration of cell lysates was determined using the Bradford method using a Quick Start Bradford Protein Assay Kit 1 (Bio-Rad Laboratories, Inc.). Proteins lysates (20 μg/lane) which were denatured using SDS-PAGE sample loading buffer (Bio-Rad Laboratories, Inc.) and were resolved by SDS-PAGE on a 10% gel and then transferred to a Hybond-P polyvinylidene fluoride membrane (Amersham; Cytiva). After blocking with 5% BSA (Sigma-Aldrich; Merck KGaA) in PBS solution at room temperature for 1 h, the membrane was first incubated with primary antibodies against TRPC7, β-actin, GFP, phosphorylated (p)-Thr286-CaMKII (p-CaMKII), CaMKII, p-Ser473-AKT (p-AKT), AKT, ERK, p-Thr202/Tyr204-ERK (p-ERK) or GAPDH at 4˚C overnight. Antibody information and the dilution ratios were described in Table SI. The membrane was then incubated with horseradish peroxidase-conjugated secondary antibodies at room temperature for 1 h. Immunoreactive proteins were visualized using enhanced chemiluminescence reagents (Amersham; Cytiva). The semi-quantification of protein expression levels was performed using ImageJ2 (National Institutes of Health).

Liquid chromatography mass spectrometry analysis. Cell lysates were collected to analyze the components by utilizing a Waters Xevo G2 qT of mass spectrometer (Waters Corporation) as previously described (13). In brief, the tryptic peptide sample was chromatographically separated on an M-class UPLC separations module (Waters Corporation) incorporating 50 femtomole tryptic digested BSA as the internally spiked protein quantification standard. Peptide was eluted through a 75 μm x 25 cm BEH C-18 column (Waters Corporation) under gradient conditions at a flow rate of 300 nl/min over 70 min at 40˚C. The mobile phase was composed of acetonitrile as the organic modifier and formic acid (0.1% v/v) for molecule protonation. Mass spectrometry was performed on a Xevo G2 qT of (Waters Corporation) instrument equipped with a nanoflow electrospray ionization interface and operated in the data-independent collection mode. Parallel ion fragmentation was switched between low (4 eV) and high (15-45 eV) energies in the collision cell and data was collected from 300 to 2,000 m/z utilizing glu-fibrinopeptide B (m/z 785.8426; Sigma-Aldrich; Merck KGaA) as the separate data channel lock mass calibrant. Data were processed using ProteinLynx GlobalServer v3.0 (Water Corporation) for qualification and Progenesis QI for proteomics (Waters Corporation) for relative quantification. Deisotoped results were evaluated for protein association and modification using the Uniprot (www.uniprot.org) human protein database.

Cell cycle analysis. TRPC7 knockdown H1299 and TRPC7-overexpressing BEAS-2B cells were collected and fixed overnight at 4˚C using 70% ethanol. After fixation, the ethanol was removed from the fixed cells by centrifugation at 800 x g for 5 min at 4˚C. The fixed cells were then incubated with 1 ml of propidium iodide (eBioscience; Thermo Fisher, Inc.) staining solution for 30 min at room temperature in the dark. The cell cycle phase distribution was determined using flow cytometry (LSR II; BD Biosciences), and quantified using BD FlowJo™ v10 software (BD Biosciences).

Invasion assay. Cell invasion assays were performed using a Transwell system (Falcon; Corning Life Sciences) as previously described (14). Briefly, Matrigel inserts containing an 8 μm pore size membrane with a thin layer of Matrigel Basement Membrane Matrix were pre-incubated with serum-free media for 2 h at 37˚C. A total of 10^5 cells were then plated in the top chamber which contained a Matrigel (250 μg/ml)-coated membrane. In the assay, cells were plated in medium without serum or growth factor, and medium supplemented with 10% FBS (Gibco; Thermo Fisher Scientific, Inc.) was placed in the lower chamber as a chemoattractant. After incubation for 36 h at 37˚C in a humidified incubator with 5% CO_2. The cells of the membrane were fixed using 3.7% formaldehyde and stained using 0.1% crystal violet (Sigma-Aldrich; Merck KGaA) at room temperature for 30 min. Cells that had not infiltrated the membrane pores were removed with a cotton swab. Images of invaded cells on the lower surface of the membrane were observed using a Ti-U bright field microscope (Nikon Corporation). In each condition, 5 independent fields were quantified using ImageJ2 (National Institutes of Health) and the average of these fields considered as the mean number of invasive cells per condition.

Calcium response assay. Intracellular Ca^{2+} responses in cells were assessed by applying 1 μM thapsigargin (TG; Sigma-Aldrich; Merck KGaA) or 100 μM

1-oleoyl-2-acetyl-sn-glycerol (OAG; Sigma-Aldrich; Merck KGaA), as previously described (7). Prior to these experiments, cells were loaded with 1 μM Fluo-4-AM (Molecular Probes; Thermo Fisher Scientific, Inc.) and incubated at 37˚C for 20 min. Intracellular Ca^{2+} concentration $[Ca^{2+}]_i$ was calculated from the ratio of fluorescence intensities (excitation/emission wavelength, 488/525 nm) using an Olympus Cell^R IX81 living cell real-time long-term fluorescence micro-imaging system (Olympus Corporation). The intracellular Ca^{2+} concentration was determined based on calibration curves as follows. A Ca^{2+} calibration curve was created using a Ca^{2+} Calibration Buffer kit (Molecular Probes; Thermo Fisher Scientific, Inc.). Intracellular Ca^{2+} ($[Ca^{2+}]_i$) was estimated from Fluo-4 excited at 488 nm and imaged using an Olympus Cell^R IX81 fluorescence microscope and UPLanApo 10x objective lens at 20˚C. Fluo-4 signals were calibrated by measuring the fluorescence intensity from microcuvettes containing 10 mM K_2-EGTA (pH 7.20) buffered to numerous $[Ca^{2+}]$ levels. Ca^{2+} concentration was analyzed using the following formula: $[Ca^{2+}]_i$=KD x (F-Fmin/Fmax-F). Plotting the fluorescence intensity versus $[Ca^{2+}]$ yielded the calibration curve with the formula of: $[Ca^{2+}]_i$=KD x (F-Fmin/Fmax-F), where KD=345 nM, F=Fluo-4 intensity, Fmax=640 and Fmin=21.7 for Fluo-4.

Cell viability. Cell viability was determined by replacing the medium from TRPC7 knockdown H1299 and TRPC7-overexpressing BEAS-2B cells on day 0, 1, 2 and 3, with MTT (Sigma-Aldrich; Merck KGaA) at a final concentration of 500 g/ml in Phenol-Red-free medium (Gibco; Thermo Fisher Scientific, Inc.) containing 10% FBS (Gibco; Thermo Fisher Scientific, Inc.). Cells were then incubated in the dark at 37˚C for 4 h. After dissolving the resulting formazan crystals through incubation with 100% DMSO at 37˚C for 5 min, the solution was transferred to a 96-well ELISA plate and quantified at 570 nm using an XS2 ELISA reader (Biotex, Inc.).

Gene Expression Omnibus (GEO) Database Analysis. GEO is a gene expression profiling database (https://www.ncbi.nlm.nih.gov/geo) (15). The GSE149507 dataset was used during analysis of the expression of *TRPC7*, *CaMKII*, *AKT*, *ERK1* and *ERK2* in 18 pairs of small cell lung cancer tumors and adjacent lung tissues which were obtained from surgical resection. Gene expression profiling was performed by microarray.

Ingenuity Pathway Analysis (IPA). QIAGEN IPA software (QIAGEN IPA Winter Release, December 2021; Ingenuity Systems, Inc.) includes a large database with thousands of biological, chemical, and medical studies. IPA also enables identification of related signaling pathways, upstream regulators, molecular interactions, disease processes and candidate biomarkers. Thus, TRPC7, CaMKII, AKT and MAPK were searched in the IPA database to clarify their relationship in signaling pathways and related diseases or functions (16).

Statistical analysis. GraphPad Prism 5.0 (GraphPad Software, Inc.; Dotmatics) was utilized to generate bar charts with error bars indicating standard deviations. One-way ANOVA followed by Bonferroni's post-hoc test and two-tailed, paired or unpaired Student's t-test were used to compare the differences between groups. Furthermore, overall patient survival was calculated from the time of surgery to the time of death or to the time of the last follow-up, at which point the data were censored. The Kaplan-Meier method was used to evaluate the difference between subgroups with high and low TRPC7 expression levels, and overall survival curves were generated. $P<0.05$ was considered to indicate a statistically significant difference.

Results

TRPC7 overexpression correlated with a lower survival rate in patients with lung adenocarcinoma. To evaluate the role of TRPC7 in the regulation of lung cancer progression, the expression of TRPC7 in paired biopsy specimens from patients with lung adenocarcinoma was first examined. The protein expression level of TRPC7 was significantly increased in tumor tissues compared with non-tumor tissues (Fig. 1A and B). This indicated that TRPC7 may serve a role in the promotion of tumor malignancy. Therefore, the clinicopathological role of TRPC7 in adenocarcinoma progression was evaluated, and the results from the TRPC7 high and low expression groups were presented (Fig. 1C). Kaplan-Meier analysis according to TRPC7 expression level indicated that patients with lung adenocarcinoma with high TRPC7 expression levels had a significantly decreased overall survival compared to those patients with low TRPC7 expression levels (P=0.002) (Fig. 1D). These results suggested that TRPC7 upregulation was associated with a worse prognosis for patients with lung adenocarcinoma.

Role of TRPC7 in the regulation of cell proliferation and cell cycle progression in lung adenocarcinoma. To evaluate the mechanism of TRPC7-mediated malignancy in lung cancer, the protein expression levels of TRPC7 in NSCLC cell lines were evaluated. The results demonstrated that there were markedly higher protein expression levels of TRPC7 in NSCLC cell lines, especially in the adenocarcinoma H1299 and A549 cells compared with the lung cell lines, BEAS-2B, BES-1A1.6 and IMR-90 (Fig. 2A). A similar result was demonstrated by the results of the proteomic analysis (Fig. 2B). As pathological features of TRPC7 are associated with tumor size in patients with lung adenocarcinoma (7), cell growth and cell cycle progression after knockdown or overexpression of TRPC7 in lung cancer cells were explored. TRPC7 was knocked down in TRPC7-overexpressing H1299 cells using TRPC7 siRNA (Fig. 2E), which markedly reduced cell proliferation (Fig. 2C). This was due to most H1299 cells being in the G0/G1 phase during TRPC7 knockdown, which indicated increased cell cycle arrest and decreased cell cycle progression in these cells (Fig. 2G). A significant decrease in the proportion of cells in the G2/M phase, compared with the si control group was also demonstrated following TRPC7 knockdown. However, overexpression of TRPC7 in BEAS-2B cells which is a lung cell line with slight TRPC7 expression, markedly increased cell proliferation (Fig. 2D) and promoted cell cycle progression with a significantly increased population of cells in the G2/M phase (Fig. 2H), compared with the control. These results supported the hypothesis that the functional role of TRPC7 in adenocarcinoma was to modulate cell growth through effects on cell cycle progression.

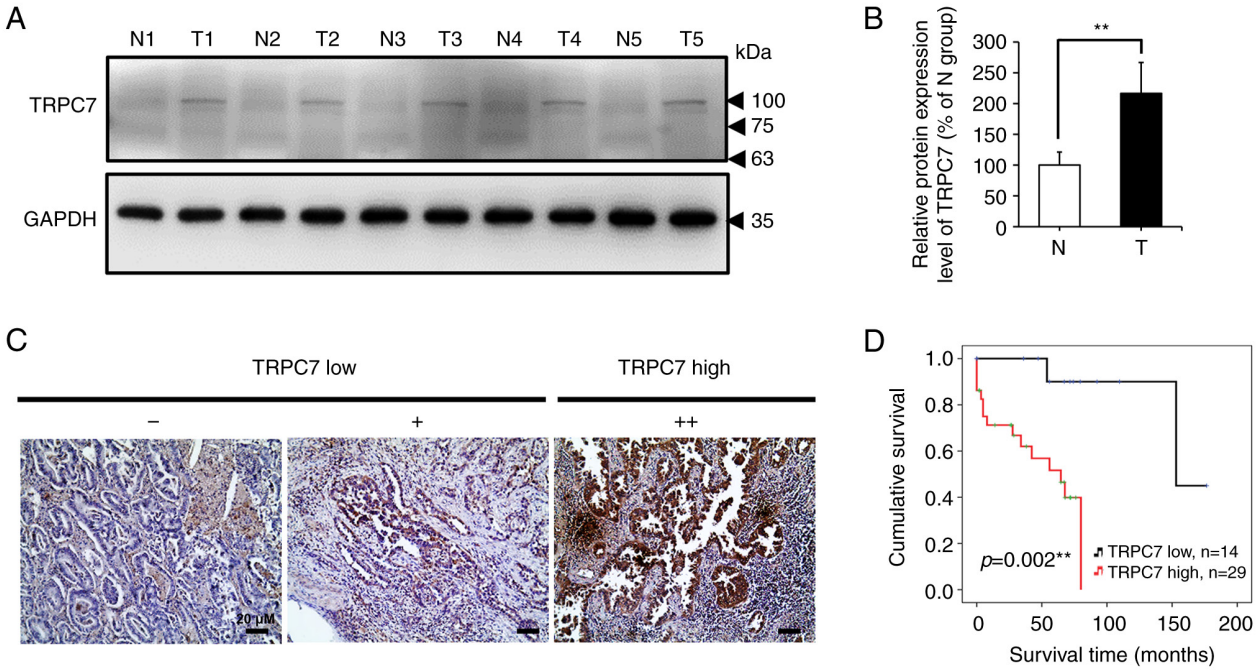

Figure 1. TRPC7 levels are significantly associated with shorter survival time in patients with lung adenocarcinoma. (A) Immunoblotting detection of the protein expression levels of TRPC7 in paired lung adenocarcinoma tissues (T) and non-tumor tissues (N). (B) Semi-quantification of the TRPC7 protein expression levels using a paired Student's t-test (mean ± SD). n=12 for each group analyzed. (C) Representative immunohistochemical staining of TRPC7 in lung adenocarcinoma tissues (magnification, x200). ++, indicated high expression of TRPC7; + or - indicated low expression of TRPC7. (D) Kaplan-Meier curves with univariate analysis for patients with low vs. high TRPC7 expression. **P<0.01. TRPC7, transient receptor potential canonical 7; T, lung adenocarcinoma tissues; N, non-tumor tissues.

TRPC7 regulates cell migration in lung adenocarcinoma. TRPC7 upregulation is closely associated with a poor prognosis in patients with lung adenocarcinoma; the metastatic tendency of cancer cells is related to malignancy and this could explain the poor prognosis of patients (17). The capacity of TRPC7 to promote cancer cell migration was assessed. TRPC7 downregulation by siRNA in H1299 cells significantly restrained cell migration (Fig. 3A) and invasion (Fig. 3B), and TRPC7 upregulation in normal lung cells significantly promoted cell migration (Fig. 3C) and invasion (Fig 3D). Consequently, the results demonstrated that TRPC7 overexpression contributed to a significant increase in cell migration in lung adenocarcinoma.

TRPC7 regulates cell growth and migration due to the increased level of Ca^{2+} influx. As Ca^{2+} signaling is crucial in the regulation of cancer cell growth and metastasis, TRPC7 channel activity was further evaluated. According to a previous study, TRPC7 can be activated by both receptor- and store-operated modes (18). Diacylglycerol (DAG) is a TRPC7 agonist that interacts with the TRPC7 receptor to induce Ca^{2+} influx; TG, an inhibitor of sarcoplasmic and endoplasmic reticular Ca^{2+} ATPase pumps, is utilized to trigger store-operated Ca^{2+} entry (SOCE). Therefore, the DAG analog, OAG, and TG were used to evaluate TRPC7 channel activity in lung cancer cells. OAG-induced Ca^{2+} influx was significantly attenuated in TRPC7 knockdown H1299 cells but was significantly promoted in TRPC7-overexpressing BEAS-2B cells compared with control cells (Fig. 4A and B and, S1A and B).

Similar results were also demonstrated for TG-induced SOCE activity. TRPC7 knockdown in H1299 cells significantly inhibited TG-induced SOCE activity compared with that in the si control group (Fig. 4C and S1C). As TRPC7 overexpression in BEAS-2B cells significantly increased SOCE activity following TG stimulation (Fig. 4D and S1D), which indicated that TRPC7 potentially regulated TG-induced SOCE activity. These data demonstrated that TRPC7-mediated cell growth and migration were Ca^{2+} signaling dependent.

CaMKII, AKT and MAPK signaling pathways are involved in TRPC7-mediated Ca^{2+} signaling. The involvement of MAPK and AKT signaling pathways in the enhancement of cell growth and migration, that leads to malignancy in cancer cells, is Ca^{2+} signaling dependent (2). IPA demonstrated that TRPC7-mediated Ca^{2+}/CaMKII, AKT and MAPK signaling pathways were associated with several diseases and cell functions, such as organismal injury and abnormalities, cancer development, post-translation modification, cellular growth, cell cycle and cell morphology (Table SII). Ca^{2+}-dependent activation of CaMKII induces the phosphorylation of AKT and ERK, which promotes cancer cell proliferation and migration (4). Therefore, the TRPC7-mediated Ca^{2+}/CaMKII/AKT and Ca^{2+}/CaMKII/ERK axes may be involved in the control of cancer progression. A similar result was also demonstrated in small cell lung cancer according to the Gene Expression Omnibus database analysis. The expression levels of *TRPC7*, *CaMKII*, *AKT*, *ERK1* and *ERK2* were significantly upregulated in tumor tissues compared to non-tumor tissues (Fig. S2). The effect of TRPC7-mediated Ca^{2+} signaling on the CaMKII, AKT and MAPK pathways was explored. The data indicated that blockade of TRPC7 expression in lung adenocarcinoma cells using siRNA and the TRPC7 inhibitors, SKF96365 and

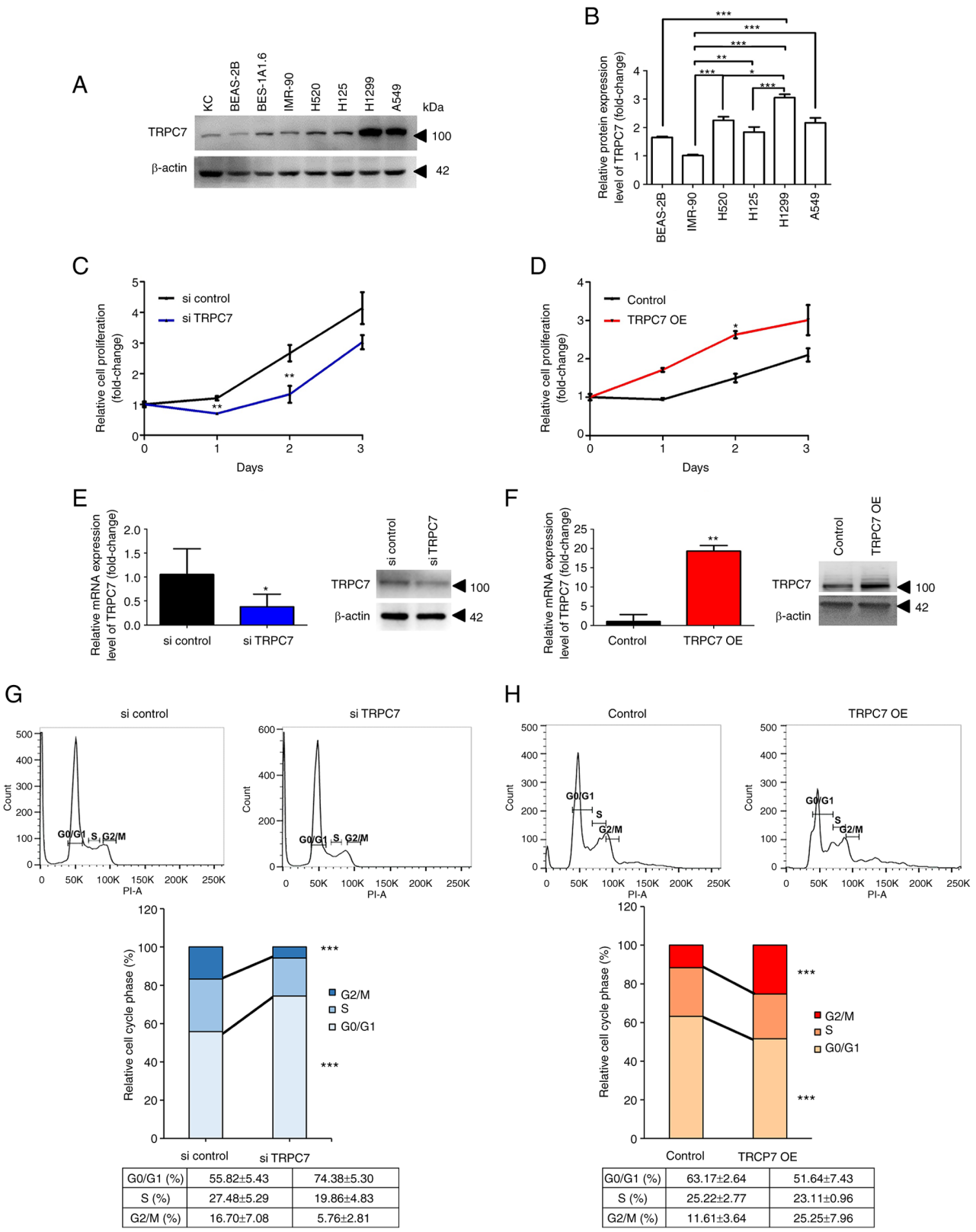

	si control	si TRPC7
G0/G1 (%)	55.82±5.43	74.38±5.30
S (%)	27.48±5.29	19.86±4.83
G2/M (%)	16.70±7.08	5.76±2.81

	Control	TRCP7 OE
G0/G1 (%)	63.17±2.64	51.64±7.43
S (%)	25.22±2.77	23.11±0.96
G2/M (%)	11.61±3.64	25.25±7.96

Figure 2. Effect of TRPC7 on cell proliferation in lung adenocarcinoma. (A) Immunoblot detection of the protein expression level of TRPC7 in lung cell lines. Normal lung cell lines were BEAS-2B (human bronchial epithelium), BES-1A1.6 (human bronchial epithelium) and IMR-90 (human lung fibroblast). Squamous cell carcinoma cell lines were H125 and H520. Adenocarcinoma cell lines were A549 and H1299. KC were used as TRPC7-positive control cells. (B) Further comparison of endogenous TRPC7 protein expression levels among normal lung, squamous cell carcinoma and adenocarcinoma cell lines using LC/MS. Quantification of the TRPC7 expression analyzed using unpaired Student's t-test. Data were presented as mean ± SD. Effect of (C) TRPC7 knockdown and (D) TRPC7 overexpression on H1299 and BEAS-2B cell proliferation (analyzed using unpaired t-test), respectively. Reverse transcription-quantitative PCR and immunoblotting analysis demonstrated that TRPC7 mRNA and protein expression levels were (E) reduced in H1299 and (F) overexpressed in BEAS-2B cells (analyzed using unpaired t-test). The percentage of (G) TRPC7 knockdown H1299 and (H) TRPC7-overexpressing BEAS-2B cells in the G0/G1, S and G2/M phases (analyzed using unpaired Student's t-test; n=3). Data were presented as mean ± SD for all experiments. *P<0.05, **P<0.01 and ***P<0.001. KC, primary normal human epidermal keratinocytes; LC/MS, liquid chromatography tandem mass spectrometry; OE, overexpression; si, small interfering RNA; TRPC7, transient receptor potential canonical 7.

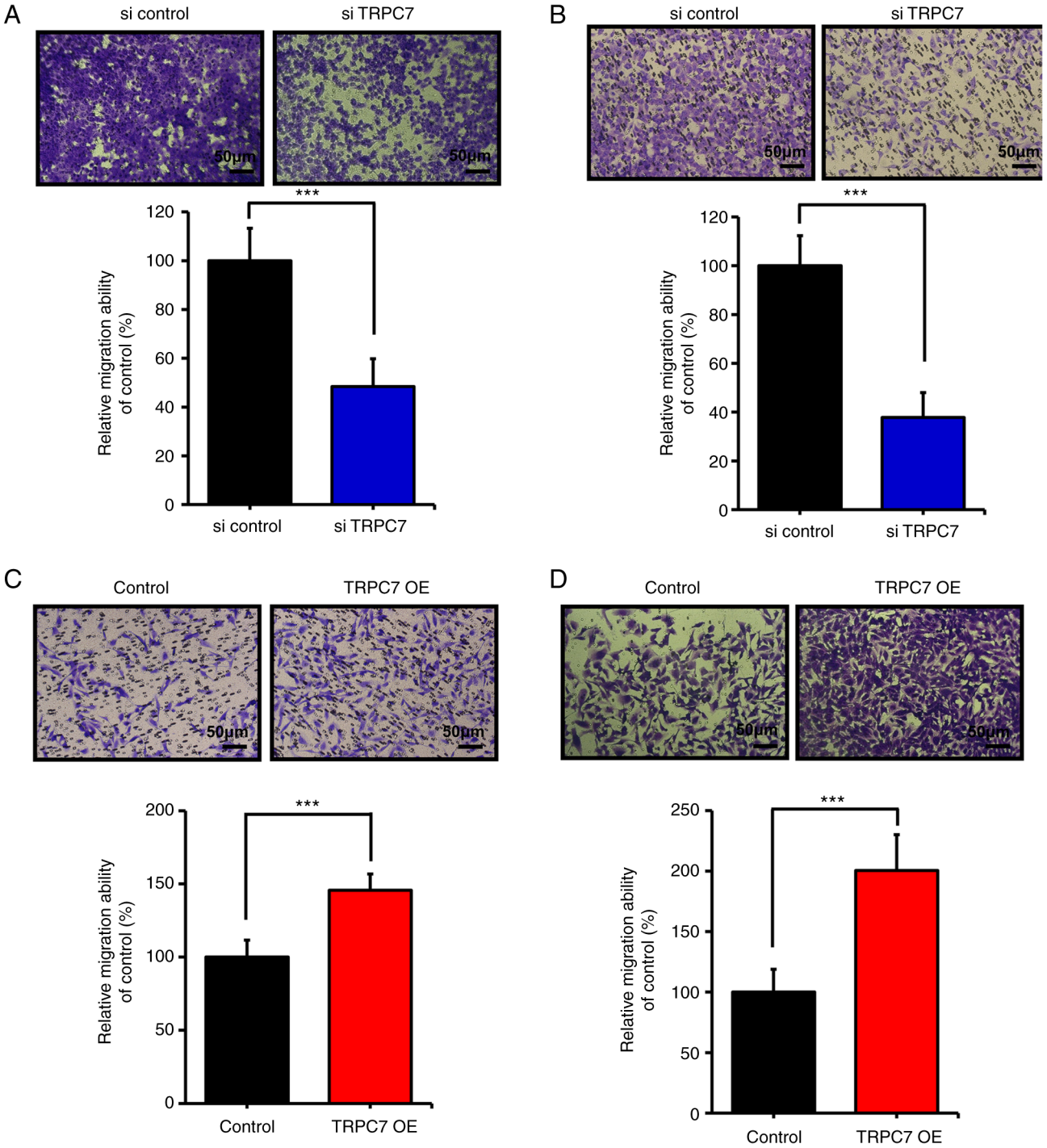

Figure 3. Effect of TRPC7 on cell migration in lung adenocarcinoma cells. Analysis of (A) cell migratory ability and (B) invasion in H1299 cells with downregulation of TRPC7. Analysis of (C) cell migratory ability and (D) invasion in BEAS-2B cells with overexpression of TRPC7 (Magnification, x200). Quantification of the migratory and invading cells analyzed using unpaired Student's t-test. n=10; Data were presented as mean ± SD. ***P<0.001. OE, overexpression; si, small interfering RNA; TRPC7, transient receptor potential canonical 7.

2-APB, significantly suppressed the activation of CaMKII, AKT and ERK as indicated by the decreased expression levels of their phosphorylated proteins, but did not influence the expression of total CaMKII, AKT and ERK (Figs. 5A, B and S3A). Furthermore, SKF96365 and 2-APB both markedly reduced the protein expression levels of p-CaMKII, p-AKT and p-ERK but not total AKT and ERK in TRPC7-overexpressing BEAS-2B cells compared with the control (Figs. 5C, D and S3B). The ratio of p-CaMKII/CaMKII, p-AKT/AKT and p-ERK/ERK was also decreased by the inhibition of TRPC7 expression (Figs. 5B and D). These results demonstrated that the activation of the AKT and MAPK signaling pathways could be dependent on TRPC7-mediated Ca^{2+}/CaMKII signaling.

To further demonstrate that TRPC7-mediated Ca^{2+} signaling was important in the regulation of cancer progression, cancer cell growth and invasion, H1299 cells where TRPC7 expression was inhibited by SKF96365, or in combination with overexpressed-TRPC7 for rescue, were evaluated.

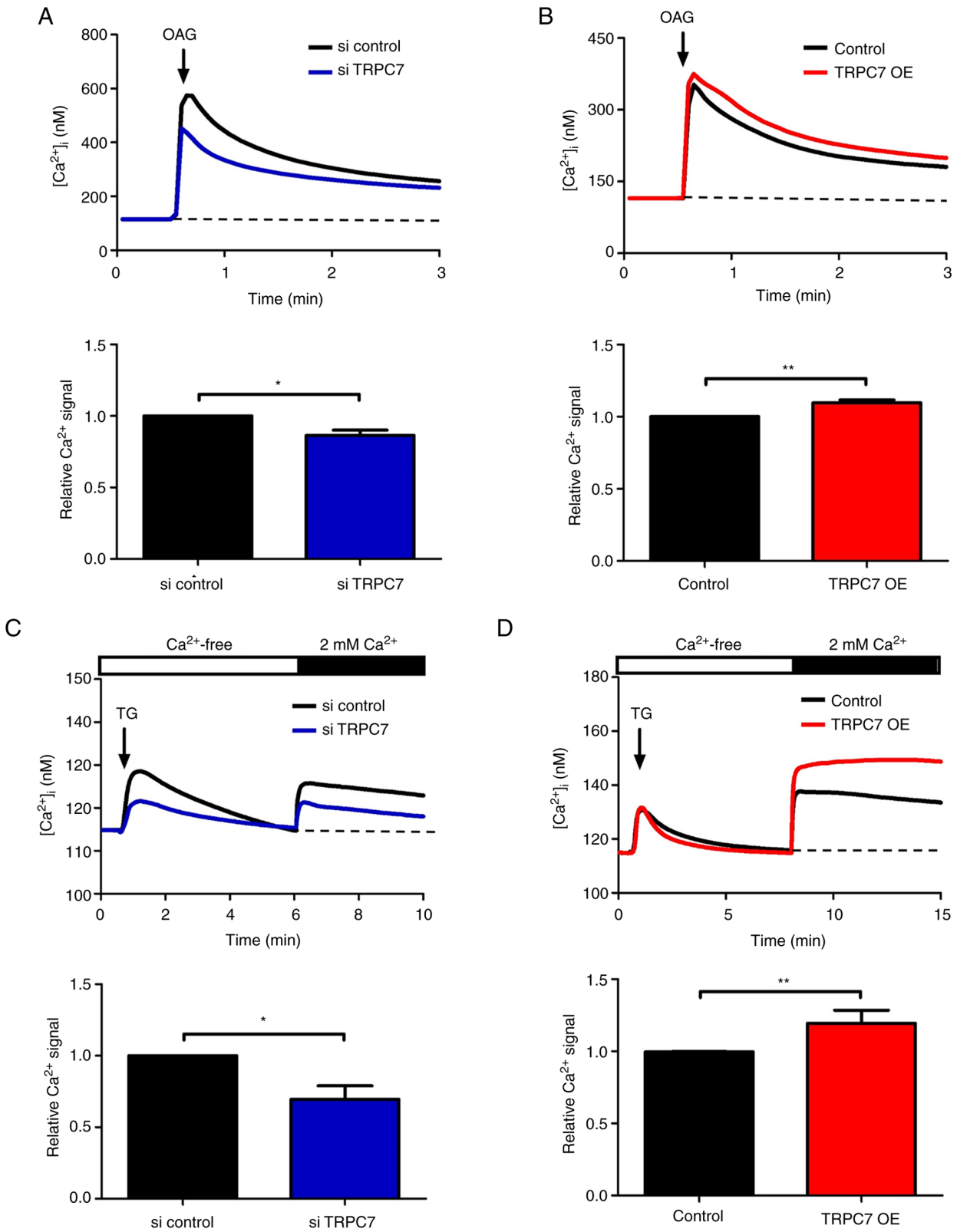

Figure 4. Effect of TRPC7 on intracellular Ca^{2+} mobilization in lung adenocarcinoma cells. Intracellular Ca^{2+} responses were measured using Ca^{2+} imaging after treating (A) TRPC7 knockdown H1299 and (B) TRPC7-overexpressing BEAS-2B cells with OAG. Lower panel: Mean area under the intracellular Ca^{2+} response curves of cells after OAG application. TG-induced Ca^{2+} influx in (C) TRPC7 knockdown H1299 and (D) TRPC7-overexpressing BEAS-2B cells. Lower panel: Mean area under the intracellular Ca^{2+} response curves after the addition of extracellular $CaCl_2$. n>100 cells; analyzed using unpaired Student's t-test. Data were presented as mean ± SD. *P<0.05 and **P<0.01. OAG, 1-oleoyl-2-acetyl-sn-glycerol; OE, overexpression; si, small interfering RNA; TG, thapsigargin; TRPC7, transient receptor potential canonical 7.

SKF96365-induced TRPC7 downregulation in H1299 cells significantly attenuated cancer cell viability and invasion compared with the control; however, overexpression of TRPC7 in H1299 cells which were pretreated with SKF96365 caused

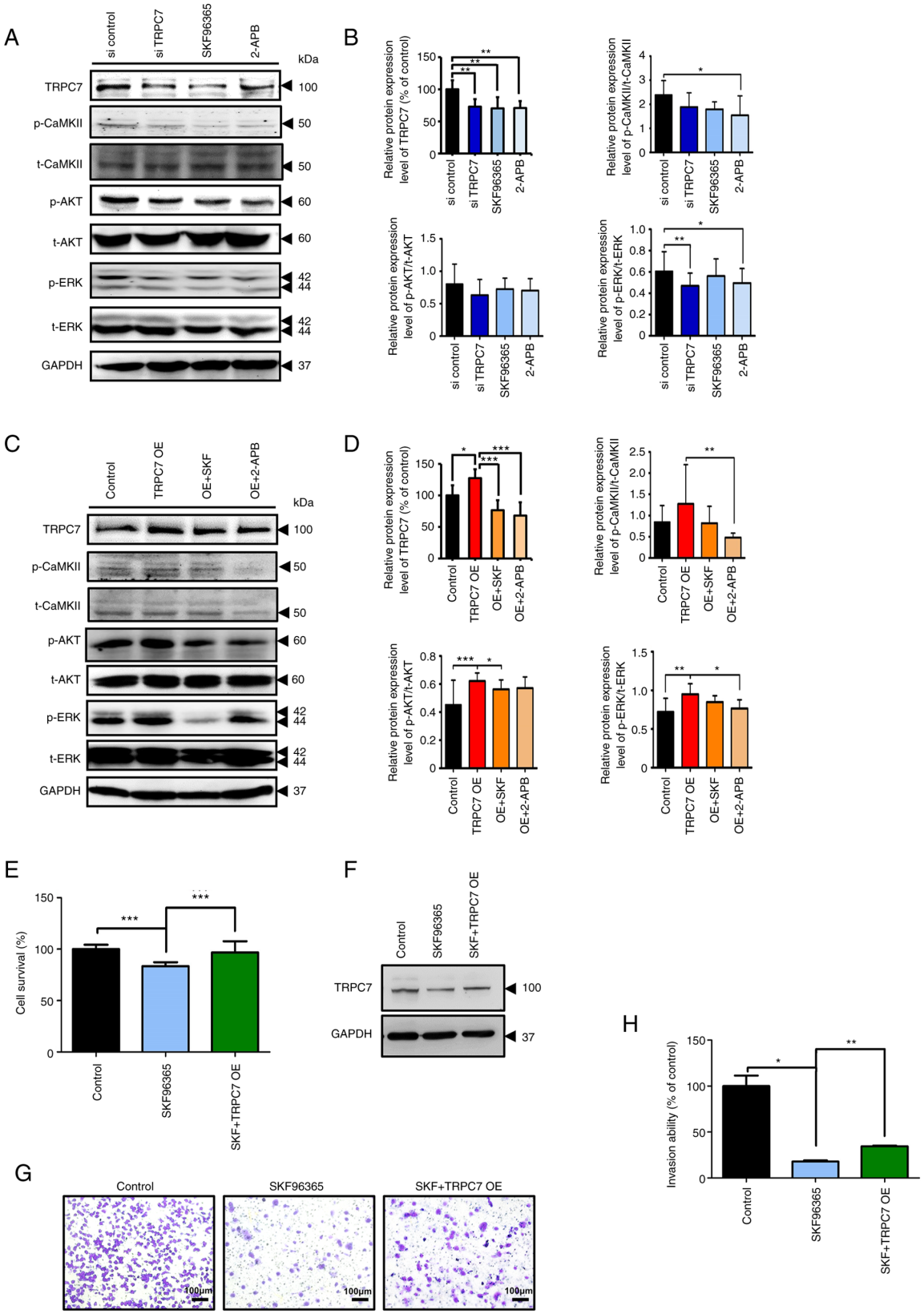

Figure 5. TRPC7 accelerates the progression of adenocarcinoma by regulating the AKT and MAPK signaling pathways. Immunoblotting analysis results demonstrated the protein expression levels of TRPC7, p-CaMKII, t-CaMKII, p-AKT, t-AKT, p-ERK, t-ERK and GAPDH in (A) TRPC7 knockdown H1299 and (C) TRPC7-overexpressing BEAS-2B cells with or without treatment with the TRPC7 inhibitors, SKF96365 and 2-APB. (B) and (D) Semi-quantification of the protein expression levels of TRPC7 and modulation of pCaMKII/CaMKII, pAKT/AKT and pERK/ERK ratios. Data were normalized to the protein expression of GAPDH as the internal control. Semi-quantification of the protein expression levels analyzed using unpaired Student's t-test. n=7, data were presented as mean ± SD. SKF96365-induced reduction of (E) cell viability, and (G) invasion ability were rescued by overexpression of TRPC7 in H1299 cells (magnification, x100). (F) Immunoblotting analysis demonstrated TRPC7 expression in H1299 cells. (H) Quantification of the invading cells, analyzed using unpaired Student's t-test. n=6, data were presented as mean ± SD. *P<0.05, **P<0.01 and ***P<0.001. 2-APB, 2-aminoethyl diphenylborinate; CaMKII, Ca^{2+}/calmodulin-dependent protein kinase II; OE, overexpression; p, phosphorylated (protein); si, small interfering RNA; SKF, SKF96365; t, total (protein); TRPC7, transient receptor potential canonical 7.

recovery (Figs. 5E-H). These findings indicated that the decrease in TRPC7-mediated Ca^{2+} signaling restrained lung adenocarcinoma cell growth and migration via interruption of the CaMKII, AKT and MAPK signaling pathways.

Discussion

A number of TRP channels have been identified using their characteristics and functions in cancers and, the role of TRPC7 in cancer progression has been independently reported; however, the clinicopathological functions of TRPC7 required further exploration. Clinical data in the present study, indicated that TRPC7 overexpression in patients with lung adenocarcinoma was associated with worse prognosis (Fig. 1). The present study also investigated the role of TRPC7 in the regulation of lung adenocarcinoma cell growth and migration via the TRPC7-mediated Ca^{2+} signaling-dependent Ca^{2+}/CaMKII/AKT and Ca^{2+}/CaMKII/ERK axes (Fig. 6). It was demonstrated that TRPC7 overexpression promoted cell cycle progression and cell migration in a lung adenocarcinoma cell line, and blockade of TRPC7-mediated Ca^{2+} signaling inhibited cancer malignancy by restraining the phosphorylation of CaMKII, AKT and ERK. These results suggested that oncogenic TRPC7 was a potential prognostic marker in lung adenocarcinoma because TRPC7 overexpression accelerates cancer malignancy. Therefore, the blocking of TRPC7 activity using SKF96365, 2-APB or TRPC7 siRNA potentially inhibits the progression of lung adenocarcinoma.

Interestingly, the ratio of p-CaMKII/CaMKII, p-AKT/AKT and p-ERK/ERK were not all significantly decreased following treatment with 2-APB or SKF96365 in the present study. For example, p-CaMKII/t-CaMKII was significantly decreased by 2-APB but not SKF96365 compared with the transfected control and p-AKT/t-AKT was significantly reduced by SKF96365 but not 2-APB compared with untransfected cells (Fig. 5B and D). It could be that SKF96365 or 2-APB may also affect other Ca^{2+} channels following effects on the signal molecules. Calcium signals are central in the mechanisms underlying cancer cell proliferation, death and migration (1). Therefore, TRPC7 may promote cancer development and TRPC6 or other TRP channels cannot be excluded from roles in the regulation of cancer development through Ca^{2+}/CaMKII/AKT and/or Ca^{2+}/CaMKII/ERK axes (5). Furthermore, cell proliferation results of the present study only demonstrated the significance at Day 2 (Fig. 2C and D); which indicated that the role of TRPC7 was specific for cell growth. The cells at Day 1 could maintain their survival when changed to the new environment for experiments and the cells at Day 3 almost filled the culture dish, which may have affected their cell division and the increase in the number of cells. It could therefore by hypothesized that the cells at Day 2 were in the logarithmic growth phase which was why a significant increase was observed at Day 2.

TRPC7 is not only a tumor initiator gene (7) but also accelerates cancer progression through the regulation of cell cycle progression and cell migration. The present study provided direct evidence that there was a relationship between oncogenic TRPC7 and TRPC7-mediated Ca^{2+} signaling-dependent CaMKII, AKT and MAPK signaling pathways in the regulation of lung adenocarcinoma malignancy (Fig. 6). There are an

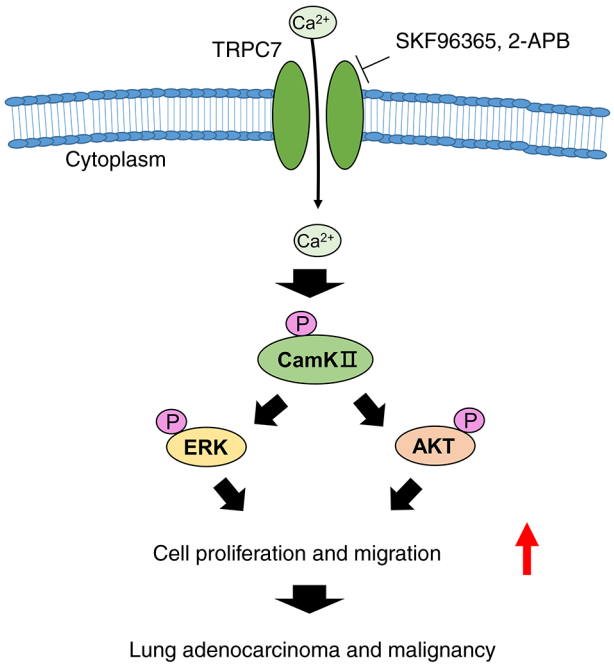

Figure 6. Schematic representation of TRPC7-mediated signaling in lung adenocarcinoma malignancy. 2-APB, 2-aminoethyl diphenylborinate; CaMKII, Ca^{2+}/calmodulin-dependent protein kinase II; p, phosphorylated (protein); TRPC7, transient receptor potential canonical 7.

increasing number of TRP channels that have been reported to promote cancer development and Ca^{2+}/CaMKII has emerged as a crucial signaling pathway in the modulation of cell proliferation, the cell cycle, invasion and metastasis, and therapy efficacy in cancer (5). For example, TRPV4 promotes oral squamous cell carcinoma cell proliferation via activation of the Ca^{2+}/CaMKII/AKT axis (19) and TRPM7 mediates breast cancer cell migration and invasion via the CaMKII-dependent MAPK signaling pathway (20). The Ca^{2+}/CaMKII/ERK axis is responsible for the phosphorylation and subsequent proteasomal degradation of cyclin-dependent kinase inhibitor 1B ($p27^{Kip1}$), which contributes to the enhancement of the S-G2/M transition of the cell cycle in colon adenocarcinoma cells (21). The results of the present study also demonstrated that overexpression of TRPC7 promoted cell cycle progression with a significant increase in the population of G2/M phase cells. $p27^{Kip1}$ may be involved in TRPC7-mediated cell cycle progression; however, this hypothesis requires assessment in future work.

AKT can directly regulate focal adhesion kinase (FAK) through the AKT-FAK interaction, which causes cancer cell adhesion and metastasis (22,23). TRP channels, such as TRP cation channel subfamily M member (TRPM)4 and TRP cation channel subfamily V member 4, enhance cell migration with activation of FAK and actin cytoskeleton reorganization (6,24). Therefore, it could be hypothesized that AKT-FAK participates in the TRPC7-mediated Ca^{2+}/CaMKII-dependent signaling pathway to enhance cancer cell mobility. In gastric cancer, TRPM2-mediated Ca^{2+}/CaMKII signaling also promotes metastasis through upregulation of NF-κB and AKT-mediated matrix metalloproteinases (MMPs) (6). The pathological role of TRPC7-mediated Ca^{2+} signaling in the regulation of lung adenocarcinoma malignancy may

therefore be related to the CaMKII/AKT/FAK and CaMKII/AKT/MMP axes.

TRPC7-mediated excess Ca^{2+} signaling in primary keratinocytes induces intracellular reactive oxygen species (ROS) accumulation, DDR and intracellular senescence following cell death (7). Notably, oncogenes induce ROS production and ROS have been reported to be mitogenic signaling molecules which mediate cancer cell hyperproliferation when DDR is activated (25). It has also been reported that TRPC7 overexpression in UVB-induced skin tumorigenesis contributed to intracellular senescence and *p53* family mutation (7). Although TRP channels are involved in oncogenic ROS production, DDR inactivation seems to be the key point for ROS-mediated cancer malignancy. It can therefore be hypothesized that TRPC7 overexpression in lung adenocarcinoma cells induces intracellular ROS accumulation through activation of mitogenic signaling, which fuels the aberrant proliferation of cells with p53 family dysfunction. Oncogenic TRPC7 promotes skin tumorigenesis and lung adenocarcinoma development (7). Accordingly, the mechanism of TRPC7-regulated malignancy does not belong to a cell-specific response and it may also apply to other types of cancer.

Furthermore, epigenetic mechanisms have been reported to promote the expression of TRP channels in cancer cells (5). Therefore, TRPC7 overexpression in lung adenocarcinoma cells may be involved in epigenetic mechanisms. As genetic variants can alter epigenetic features and epigenetic variations can mediate genetic variability (26), TRPC7 may possess specific gene polymorphisms which are correlated with lung cancer development. A study of the identification of *TRPC* genetic variants in the Chinese population by Zhang *et al* (27) reported that *TRPC4 rs9547991* and *rs978156*, and *TRPC7 rs11748198* were candidate susceptibility markers for lung cancer. The association of *TRPC7 rs11748198* with lung cancer risks may be due to changes in the epigenetic features that cause upregulation of TRPC7 expression in lung cancer. Although the present study demonstrated the mechanism of TRPC7 in cancer development, it is still unclear whether TRPC7 can affect epigenetic regulation to promote cancer malignancy. The effect of *TRPC7 rs11748198* on lung cancer progression requires validation in future studies.

Overall, to the best of our knowledge, the present study was the first to demonstrate the pathological role of TRPC7 in the regulation of cancer progression. High TRPC7 expression was associated with a worse prognosis for patients with lung adenocarcinoma and modulated the growth and migration of lung adenocarcinoma cells through the activation of TRPC7-mediated Ca^{2+} signaling-dependent CaMKII, AKT and MAPK pathways. The present study increased understanding of the precise role served by TRPC7 in cancer malignancy and could provide a novel therapeutic molecular target for patients with lung adenocarcinoma.

Acknowledgements

The authors would like to thank the Center for Research Resources and Development at Kaohsiung Medical University (Kaohsiung, Taiwan) for the use of the confocal microscope, the Olympus Cell-R IX81 fluorescence microscope and the LSR II flow cytometer.

Funding

The present study was supported by the Ministry of Science and Technology of Taiwan (grant no. MOST 109-2314-B-037-143 and MOST 110-2314-B-037-035), Kaohsiung Municipal Ta-Tung Hospital, Kaohsiung Medical University Hospital (grant no. kmtth-110-R003) and Chi Mei Medical Center (grant no. CLFHR10509 and CLFHR10709).

Availability of data and materials

The datasets used and/or analyzed during the current study are available from the corresponding author on reasonable request.

Authors' contributions

JLL and WLH were responsible for conceptualization. JLL, YCH, YFL and WLH were responsible for clinical data curation. JLL and WLH were responsible for funding acquisition. MHT performed the liquid chromatography mass spectrometry; YCH and HSL performed the immunoblot analysis and RT-qPCR; SWC performed the invasion assay; YYH, LCL, TFT performed the cell cycle analysis and cell viability assay; YFL performed the immunoblot analysis and GEO database analysis; WLH performed the calcium response assay and IPA. MHT, YCH and WLH were responsible for the methodology. HSL and YFL confirmed the authenticity of the data. JLL and WLH were responsible for writing the original draft. WLH was responsible for reviewing and editing the manuscript. All authors read and approved the final version of the manuscript.

Ethics approval and consent to participate

This study was approved by the Institutional Review Board of Chi-Mei Medical Center, (Tainan, Taiwan; approval no. 10405-L01). Written informed consent was obtained from all individual participants included in the study.

Patient consent for publication

Not applicable.

Competing interests

The authors declare that they have no competing interests.

References

1. Bong AHL and Monteith GR: Calcium signaling and the therapeutic targeting of cancer cells. Biochim Biophys Acta Mol Cell Res 1865: 1786-1794, 2018.
2. Apati A, Janossy J, Brozik A, Bauer PI and Magocsi M: Calcium induces cell survival and proliferation through the activation of the MAPK pathway in a human hormone-dependent leukemia cell line, TF-1. J Biol Chem 278: 9235-9243, 2003.
3. Gocher AM, Azabdaftari G, Euscher LM, Dai S, Karacosta LG, Franke TF and Edelman AM: Akt activation by Ca(2+)/calmodulin-dependent protein kinase kinase 2 (CaMKK2) in ovarian cancer cells. J Biol Chem 292: 14188-14204, 2017.
4. Villalobo A and Berchtold MW: The role of calmodulin in tumor cell migration, invasiveness, and metastasis. Int J Mol Sci 21: 765, 2020.

5. Hsu WL, Noda M, Yoshioka T and Ito E: A novel strategy for treating cancer: Understanding the role of Ca(2+) signaling from nociceptive TRP channels in regulating cancer progression. Explor Target Antitumor Ther 2: 401-415, 2021.
6. Yang D and Kim J: Emerging role of transient receptor potential (TRP) channels in cancer progression. BMB Rep 53: 125-132, 2020.
7. Hsu WL, Tsai MH, Wu CY, Liang JL, Lu JH, Kahle JS, Yu HS, Yen CJ, Yen CT, Hsieh YC, *et al*: Nociceptive transient receptor potential canonical 7 (TRPC7) mediates aging-associated tumorigenesis induced by ultraviolet B. Aging Cell 19: e13075, 2020.
8. Molina JR, Yang P, Cassivi SD, Schild SE and Adjei AA: Non-small cell lung cancer: Epidemiology, risk factors, treatment, and survivorship. Mayo Clin Proc 83: 584-594, 2008.
9. Jiang HN, Zeng B, Zhang Y, Daskoulidou N, Fan H, Qu JM and Xu SZ: Involvement of TRPC channels in lung cancer cell differentiation and the correlation analysis in human non-small cell lung cancer. PLoS One 8: e67637, 2013.
10. Edge SB and Compton CC: The American joint committee on cancer: The 7th edition of the AJCC cancer staging manual and the future of TNM. Ann Surg Oncol 17: 1471-1474, 2010.
11. Varghese F, Bukhari AB, Malhotra R and De A: IHC Profiler: An open source plugin for the quantitative evaluation and automated scoring of immunohistochemistry images of human tissue samples. PLoS One 9: e96801, 2014.
12. Livak KJ and Schmittgen TD: Analysis of relative gene expression data using real-time quantitative PCR and the 2(-Delta Delta C(T)) method. Methods 25: 402-408, 2001.
13. Wu CY, Hsu WL, Tsai MH, Liang JL, Lu JH, Yen CJ, Yu HS, Noda M, Lu CY, Chen CH, *et al*: Hydrogen gas protects IP3Rs by reducing disulfide bridges in human keratinocytes under oxidative stress. Sci Rep 7: 3606, 2017.
14. Hsu WL, Chung PJ, Tsai MH, Chang CL and Liang CL: A role for Epstein-Barr viral BALF1 in facilitating tumor formation and metastasis potential. Virus Res 163: 617-627, 2012.
15. Clough E and Barrett T: The gene expression omnibus database. Methods Mol Biol 1418: 93-110, 2016.
16. Thomas S and Bonchev D: A survey of current software for network analysis in molecular biology. Hum Genomics 4: 353-360, 2010.
17. Fares J, Fares MY, Khachfe HH, Salhab HA and Fares Y: Molecular principles of metastasis: A hallmark of cancer revisited. Signal Transduct Target Ther 5: 28, 2020.
18. Lievremont JP, Bird GS and Putney JW Jr: Canonical transient receptor potential TRPC7 can function as both a receptor- and store-operated channel in HEK-293 cells. Am J Physiol Cell Physiol 287: C1709-C1716, 2004.
19. Fujii S, Tajiri Y, Hasegawa K, Matsumoto S, Yoshimoto RU, Wada H, Kishida S, Kido MA, Yoshikawa H, Ozeki S and Kiyoshima T: The TRPV4-AKT axis promotes oral squamous cell carcinoma cell proliferation via CaMKII activation. Lab Invest 100: 311-323, 2020.
20. Dhennin-Duthille I, Gautier M, Korichneva I and Ouadid-Ahidouch H: TRPM7 involvement in cancer: A potential prognostic factor. Magnes Res 27: 103-112, 2014.
21. Wang YY, Zhao R and Zhe H: The emerging role of CaMKII in cancer. Oncotarget 6: 11725-11734, 2015.
22. More SK, Vomhof-Dekrey EE and Basson MD: ZINC4085554 inhibits cancer cell adhesion by interfering with the interaction of Akt1 and FAK. Oncol Lett 17: 5251-5260, 2019.
23. Wang S and Basson MD: Akt directly regulates focal adhesion kinase through association and serine phosphorylation: Implication for pressure-induced colon cancer metastasis. Am J Physiol Cell Physiol 300: C657-C670, 2011.
24. Fels B, Bulk E, Petho Z and Schwab A: The role of TRP channels in the metastatic cascade. Pharmaceuticals (Basel) 11: 48, 2018.
25. Ogrunc M, Di Micco R, Liontos M, Bombardelli L, Mione M, Fumagalli M, Gorgoulis VG and d'Adda di Fagagna F: Oncogene-induced reactive oxygen species fuel hyperproliferation and DNA damage response activation. Cell Death Differ 21: 998-1012, 2014.
26. Leung A, Schones DE and Natarajan R: Using epigenetic mechanisms to understand the impact of common disease causing alleles. Curr Opin Immunol 24: 558-563, 2012.
27. Zhang Z, Wang J, He J, Zeng X, Chen X, Xiong M, Zhou Q, Guo M, Li D and Lu W: Identification of TRPCs genetic variants that modify risk for lung cancer based on the pathway and two-stage study. Meta Gene 9: 191-196, 2016.